

# Mechanism of Nanotubular Ta<sub>2</sub>O<sub>5</sub> *via* Anodization in NH<sub>4</sub>F/H<sub>2</sub>SO<sub>4</sub>/H<sub>2</sub>O Solution

Mahzaton Aqma Abu Talip, Rozina Abdul Rani, Rosmalini Ab Kadir, Mohamad Hafiz Mamat, Muhammad Farid Abdul Khalid, Mohamad Rusop Mahmood, Ahmad Sabirin Zoolfakar.

**Abstract**—The main subject of many studies in anodization of Ta<sub>2</sub>O<sub>5</sub> is to investigate the role of electrolyte composition on nanostructure Ta<sub>2</sub>O<sub>5</sub> formation. However, the simple and clear explanation on how electrolyte composition affects the mechanism of nanotubular formation is hardly to be found. In this paper, we provided organized and step by step discussion on how NH<sub>4</sub>F, H<sub>2</sub>O and H<sub>2</sub>SO<sub>4</sub> influence the growth of nanotubular by performing the experiments with different concentration of NH<sub>4</sub>F, H<sub>2</sub>O and H<sub>2</sub>SO<sub>4</sub>. The electrochemical formation of nanotubular tantalum pentoxide (Ta<sub>2</sub>O<sub>5</sub>) was investigated in 50 ml ethylene glycol (EG), 0.5–3 wt% of NH<sub>4</sub>F, 0–6 vol% of H<sub>2</sub>O and 0–1 vol% of H<sub>2</sub>SO<sub>4</sub>. Depending on electrolyte concentration, Ta<sub>2</sub>O<sub>5</sub> films exhibit different structural structures and features after anodization. The results were shown through FESEM, real images of samples and XRD analysis. By varying the concentration, it was possible to change the structures of Ta<sub>2</sub>O<sub>5</sub>. Finally, we demonstrated how electrochemical response during anodization, thus forming nanotubular Ta<sub>2</sub>O<sub>5</sub>.

**Index Terms**—anodization, electrochemical, metal oxide, nanotubular, tantalum, Ta<sub>2</sub>O<sub>5</sub>

## I. INTRODUCTION

IN recent years, a numbers of studies on nanotubular oxide films synthesized *via* anodization have been published, for instance Al [1], [2], Ti [3], [4], Zr [5], [6], Nb [7], [8] and W [9], [10]. Another type of oxide films which we introduced in this study is tantalum pentoxide (Ta<sub>2</sub>O<sub>5</sub>). Although studies on obtaining nanotubular Ta<sub>2</sub>O<sub>5</sub> *via* anodization is limited, the interest on synthesizing nanostructure Ta<sub>2</sub>O<sub>5</sub> with variety of methods are steadily increasing, for example; one-pot hydrolysis method [11], sol-gel method [12], endo-templating method [13], facile hydrothermal method [14] etc. This is due to the fact that tantalum oxide is a versatile metal oxide, which has been used in a wide range of application; microelectronics [15], fuel cells [16], photonics [17], photocatalyst [18] and sensors [19], [20]. Ta<sub>2</sub>O<sub>5</sub> is as wide band-gap metal oxide with band-gap of 3.9 – 4.0 eV [21]. It is regard as new favorable oxide metal thanks to its resistance towards corrosion which

make it widely use in coating industry [22], [23] and its great dielectric properties which make it suitable as storage capacitors [24], [25].

In the past several years, nanotubular metal oxide has drawn a great deal of attention owing to its physical properties and potential applications [6], [8], [10]. Previous studies shows that nanotubular offers utmost advantages, by providing a direct and fast pathway for transporting electrons, thus increases the electron lifetimes in semiconductor [26], [27]. For this reason, the fabrication of nanotubular Ta<sub>2</sub>O<sub>5</sub> structures is likely to be promising for many applications. Anodization is a pronounced process for the production of an oxide films on metal oxide such as Ta. In this process, electrical current (field) or voltage is applied and electrochemical reactions will occur on the surface of metal electrode. An oxide film will then form with various morphologies such as nanotubular structure. Anodization is widely used because the method is controllable, reproducible results and the credibility to tune the size and shape of nanotubular to the wanted dimensions. In addition, the method is cost effective and the thickness and morphology of Ta<sub>2</sub>O<sub>5</sub> films can easily be controlled by manipulating the parameters [28], [29].

Up to this date, the main subject of many studies in anodization of Ta<sub>2</sub>O<sub>5</sub> is to investigate the role of electrolyte composition on nanostructure Ta<sub>2</sub>O<sub>5</sub> formation; electrolyte containing acetic acid and hydrogen or phosphoric acid [30], electrolyte with additive such as H<sub>3</sub>PO<sub>4</sub> and dimethyl sulfoxide [31], electrolyte with H<sub>2</sub>SO<sub>4</sub> + HF [32]–[34] etc. However, the mechanism of anodization on nanotubular Ta<sub>2</sub>O<sub>5</sub> formation is still the matter of investigation. The formation of structures or pattern in the electrochemical synthesis of materials is a valuable topic. Therefore, a clear-cut investigation and explanation on nanotubular Ta<sub>2</sub>O<sub>5</sub> formation. mechanism is needed.

This paper is submitted on 5<sup>th</sup> October 2018 and accepted on 14<sup>th</sup> December 2018. This work was financially supported by 600-IRMI/MyRA

Mahzaton Aqma Abu Talip is with the Faculty of Electrical Engineering, Universiti Teknologi MARA, 40450 Shah Alam, Malaysia (mahzaton08@yahoo.com).

Rozina Abdul Rani is under NANO-SciTech Centre (NST), Institute of Science (IOS), Universiti Teknologi MARA, 40450 Shah Alam, Malaysia.

Rosmalini Ab Kadir is with Faculty of Electrical Engineering, Universiti Teknologi MARA, 40450 Shah Alam, Malaysia (rosma391@salam.uitm.edu.my).

Mohamad Hafiz Mamat is under NANO-ElecTronic Center (NET), Faculty of Electrical Engineering, Universiti Teknologi MARA (UiTM), 40450 Shah Alam, Malaysia (mhmamat@salam.uitm.edu.my).

Muhammad Farid Abdul Khalid is under Microwave Research Institute, Faculty of Electrical Engineering, Universiti Teknologi MARA, 40450 Shah Alam, Malaysia (mfarid@salam.uitm.edu.my)

Mohamad Rusop Mahmood is under NANO-SciTech Centre (NST), Institute of Science (IOS) and NANO-ElecTronic Center (NET), Faculty of Electrical Engineering, Universiti Teknologi MARA, 40450 Shah Alam, Malaysia (rusop@salam.uitm.edu.my).

Ahmad Sabirin Zoolfakar is under NANO-ElecTronic Center (NET), Faculty of Electrical Engineering, Universiti Teknologi MARA (UiTM), 40450 Shah Alam, Malaysia (ahmad074@salam.uitm.edu.my).

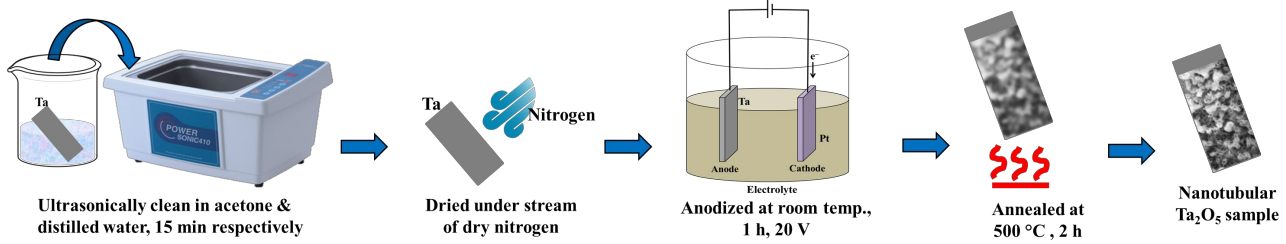


Fig. 1 Schematic illustration of cleaning, anodizing and annealing process of nanotubular Ta<sub>2</sub>O<sub>5</sub> sample.

For that reasons, in this paper, we will present the results of an experimental investigation on anodization of nanotubular Ta<sub>2</sub>O<sub>5</sub> in electrolyte mixture consisting of H<sub>2</sub>SO<sub>4</sub>, NH<sub>4</sub>F, H<sub>2</sub>O and EG. We will manipulate the concentration of H<sub>2</sub>SO<sub>4</sub>, NH<sub>4</sub>F, and H<sub>2</sub>O and discuss its role and effect on nanotubular Ta<sub>2</sub>O<sub>5</sub> formation in details through structural characterization via FESEM and XRD.

## II. METHODOLOGY

### A. Material

Ethylene glycol (EG) (purity >99.5%), NH<sub>4</sub>F (purity >98%) and H<sub>2</sub>SO<sub>4</sub> (purity >98%) were analytical grade and used without further purification. All reagents were purchased from Friendemann Schmidt and J.T Baker®. The solutions were prepared with distilled water (*Mili-Q*, resistivity of 18.2 MΩ•cm). Tantalum (Ta) foils (purity >99.95%, 0.25 mm thickness, 1.0 × 2.5 cm) were used as anode pole. Platinum (Pt) gauze (purity, 99%) was used as cathode pole. Both electrodes were purchased from Sigma Aldrich.

### B. Fabrication of nanotubular Ta<sub>2</sub>O<sub>5</sub>

Prior to anodization, Ta foil was cleaned ultrasonically for 15 minutes in acetone and distilled water, respectively. Next, Ta foil was dried under stream of dry nitrogen. Electrolytes were prepared by mixing 50 ml ethylene glycol (EG) with 0.5–3 wt% of NH<sub>4</sub>F, 0–6 vol% of distilled water and 0–1 vol% of H<sub>2</sub>SO<sub>4</sub>. Then, anodization was executed; Ta foil as anode and Pt as cathode were anodized in electrolytes at ambient temperature for 1 h. The samples were anodized at constant voltage of 20 V during each experiment. Samples were annealed after anodization at a temperature of 500 °C for 2 h with ramp up and down rate of 5 °C/min. Schematic illustration in Fig. 1 shows cleaning, anodizing and annealing process of nanotubular Ta<sub>2</sub>O<sub>5</sub> while Fig. 2 displayed the anodization set-up used in laboratory.

### C. Structural characterization

Field emission scanning electron microscope (FESEM; JEOL JSM-7600F) was used to characterize the morphological properties of the Ta<sub>2</sub>O<sub>5</sub> samples. X-Ray diffractometer (XRD; PANalytical X'Pert PRO) was used to characterize the crystallinity properties of nanotubular Ta<sub>2</sub>O<sub>5</sub>.

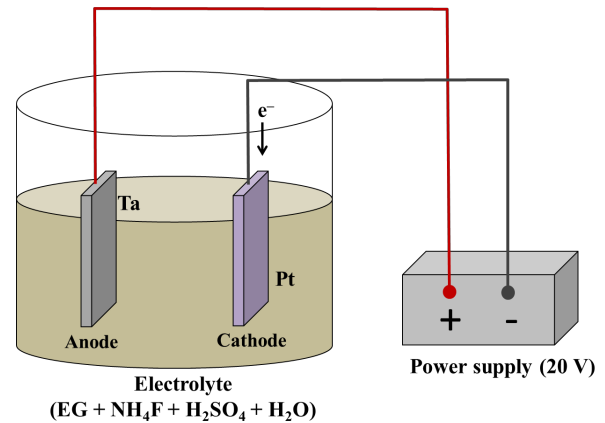


Fig. 2 Schematic set-up of nanotubular Ta<sub>2</sub>O<sub>5</sub> anodization experiments in which two electrodes are used: cathode (Pt gauze) and anode (Ta foil) with different concentration of electrolytes. Samples were anodized for 1 h with voltage bias of 20 V.

## III. RESULT AND DISCUSSION

In order to study the effect of electrolyte parameters on nanotubular Ta<sub>2</sub>O<sub>5</sub> morphology during anodization, we varied the concentration of NH<sub>4</sub>F, H<sub>2</sub>O and H<sub>2</sub>SO<sub>4</sub>. As a baseline, we referred to Hongbin *et al.* [35] where they anodized Ta foil for 1 h with bias voltage of 20 V in electrolyte which consists of EG, 3% of NH<sub>4</sub>F, 10% of H<sub>2</sub>O and 0.25% of H<sub>3</sub>PO<sub>4</sub>. Instead of using H<sub>3</sub>PO<sub>4</sub>, we used H<sub>2</sub>SO<sub>4</sub> in our experiments.

### A. Optimization of NH<sub>4</sub>F concentration in electrolyte

In past studies, it has been uncovered that the presence of fluoride ions in the electrolyte triggered the disintegration of oxide film on metal oxide and help nanostructured development [30], [36], [37]. Fluoride ions have the ability to form water-soluble complexes, and due to their small ion radius its can penetrate and compete more easily through the growing Ta<sub>2</sub>O<sub>5</sub> lattice [36]. Therefore, these abilities lead to a continuous dissolution of Ta<sub>2</sub>O<sub>5</sub>. When the balance between oxidation and dissolution is reached, a nanostructured surface form. However, nanostructures cannot form on the initial compact oxide layer if the amount of fluoride ions in the electrolyte is inadequate.

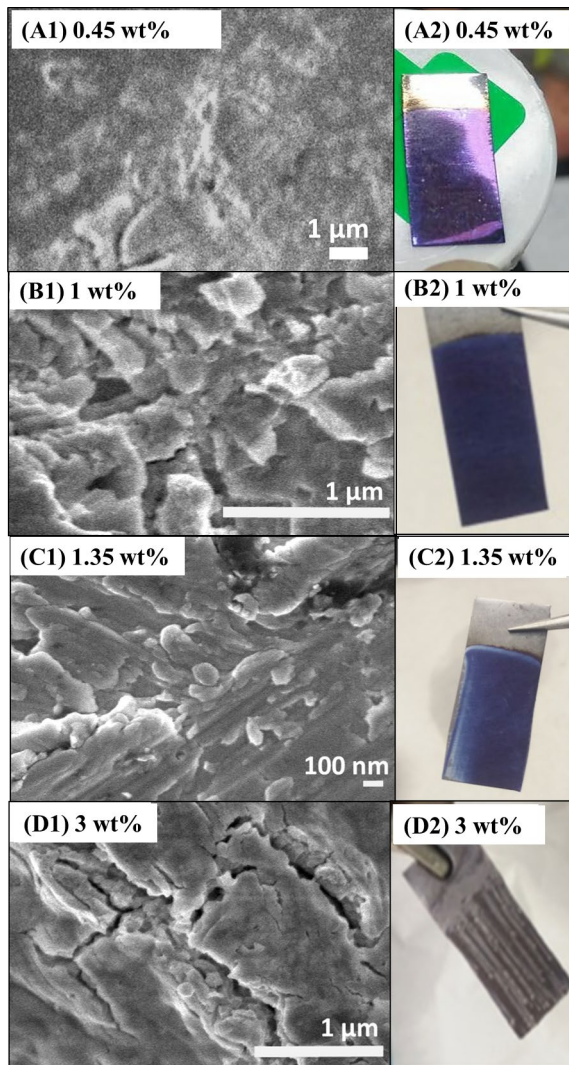


Fig. 3 FESEM and samples images after anodization in different concentration of NH<sub>4</sub>F; (A1)(A2) 0.45 wt% NH<sub>4</sub>F, (B1)(B2) 1 wt% NH<sub>4</sub>F, (C1)(C2) 1.35 wt% NH<sub>4</sub>F and (D1)(D2) 3 wt% NH<sub>4</sub>F

Contrarily, an earlier study reported that an excessive amount of fluoride ions in the electrolyte can partially damage the nanostructured network due to over-etching by fluoride ions [37].

The effect of fluoride ions on nanotubular formation during anodization was investigated by using 0.45 wt% (sample A), 1.0 wt% (sample B), 1.35 wt% (sample C) and 3.0 wt% (sample D) of NH<sub>4</sub>F in electrolyte. The concentrations of EG (50 mL), H<sub>2</sub>O (10 vol%) and H<sub>2</sub>SO<sub>4</sub> (0.25 vol%) in electrolyte were consistence. Fig. 3(A1) illustrates that there are no nanostructures formed on sample A and Fig. 3(A2) shows that sample changed into dark blue colour. Fig. 3(B1) and (B2) shows similar observations on sample B. These indicated that 0.45 wt% and 1 wt% of NH<sub>4</sub>F was insufficient to produce enough ion fluoride in electrolyte, thus no nanostructured Ta<sub>2</sub>O<sub>5</sub> was created. We also discovered that dark blue colour on sample can be determined as one of the sign that anodization layer is too thin and fail to form nanostructures on Ta foil.

Similarly, it can be seen from Fig. 3(C1) and Fig. 3(C2) that there were also no nanostructures produced and sample C shows colour change, where it turned into dark blue colour. It is apparent from these results that 1.35 wt% of NH<sub>4</sub>F still produced too few fluoride ions. The insufficiency of fluoride ions in electrolyte were thought to be caused by high water content, with a high volume of water exhibiting a lower dissolution rate. As a result tantalum oxide did not dissolve and compact oxide films were formed.

On top of that, it can be seen from Fig. 3(D1) that there are no nanostructures forming on sample. Instead of the colour change, Fig. 3(D2) shows that the sample D has been excessively etched and damaged. This analysis found evidence that 3 wt% of NH<sub>4</sub>F or more produce an excessive amount of fluoride ions and destroy nanostructure Ta<sub>2</sub>O<sub>5</sub> on sample. The summary of these experiments is shown in Table 1.

**Table 1**

Summary of the anodization experiments with different concentration of NH<sub>4</sub>F.

Experiment	EG (ml)	NH <sub>4</sub> F (wt%)	H <sub>2</sub> O (vol%)	H <sub>2</sub> SO <sub>4</sub> (vol%)	Observation
Baseline	50	3.0	10	0.25 H <sub>3</sub> PO <sub>4</sub>	
Sample A	50	0.45	10	0.25	No structure. Dark blue colour Smooth surface
Sample B	50	1.0	10	0.25	No structure. Dark blue colour Smooth surface
Sample C	50	1.35	10	0.25	No structure Dark blue colour Smooth surface
Sample D	50	3.0	10	0.25	No structure Sample damaged

### B. Optimization of H<sub>2</sub>O concentration in electrolyte

As noted in previous investigations, the addition of H<sub>2</sub>O in the electrolyte leads to the formation of compact oxide layer [38]. Previous study described H<sub>2</sub>O as “passivator” and suggested that H<sub>2</sub>O must be added in electrolyte as low as possible [35].

The influence of H<sub>2</sub>O content on nanotubular formation was explored by using 0 vol% (sample E), 2.0 vol% (sample F), 4.0 vol% (sample G) and 6.0 vol% (sample H) of H<sub>2</sub>O in electrolyte. The concentrations of EG (50 mL), NH<sub>4</sub>F (1.35 wt%) and H<sub>2</sub>SO<sub>4</sub> (0.25 vol%) in electrolyte were consistence. It can be seen from Fig. 4(E1) and (E2) that no nanostructured was produced without the presence of H<sub>2</sub>O. In the presence of 2 vol% H<sub>2</sub>O the nanotubular structure began to form, but imperfect. The anodic layer began to slit and crack, indicating that nanotubular were taking shape, as can be seen in Fig. 4(F1). Moreover, the sample changed colour to pink and the surface became rough (Fig. 4(F2)).

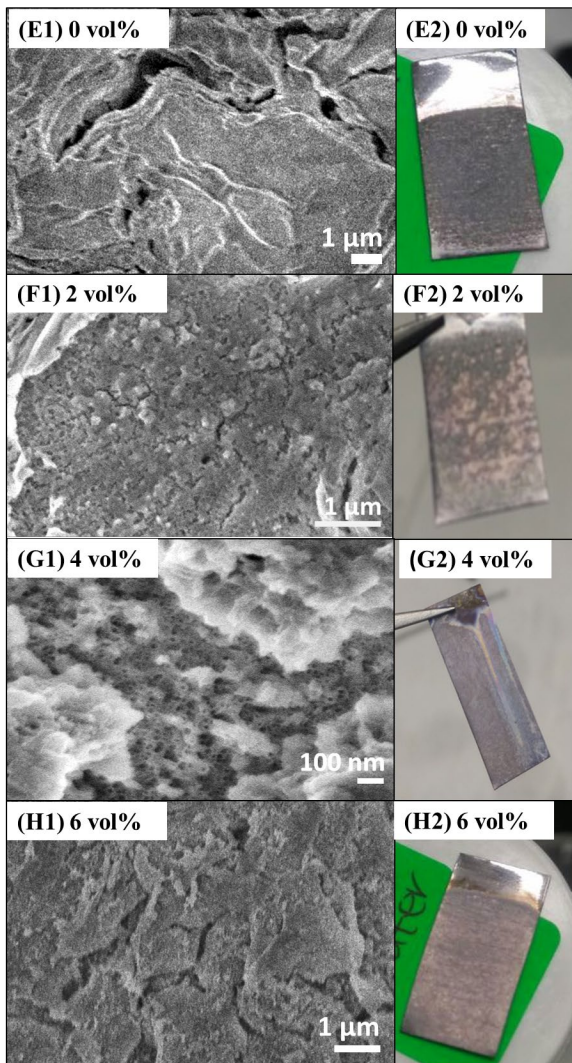


Fig. 4 FESEM and samples images after anodization in different concentration of H<sub>2</sub>O; (E1)(E2) 0 vol% H<sub>2</sub>O, (F1)(F2) 2 vol% H<sub>2</sub>O, (G1)(G2) 4 vol% H<sub>2</sub>O and (H1)(H2) 6 vol% H<sub>2</sub>O

The results in Fig. 4(F1) and (F2) have confirmed that the addition of a small amount of H<sub>2</sub>O helps to promote the formation of Ta<sub>2</sub>O<sub>5</sub> and conversely, to suppress its dissolution. While this may be true, the results also showed that when the volume of H<sub>2</sub>O was too low, the dissolution rate required for the formation of nanotubular was limited, implying that the dissolution cannot be carried out continuously. Consequently, nanotubular could not achieve their final shape as seen in Fig. 4(F1).

Therefore, volume of H<sub>2</sub>O was slightly increase more than 2 vol% and this deliver significantly better result. As shown in Fig. 4(G1) where 4 vol% of H<sub>2</sub>O was used, more apparent nanotubular structures with noticeable white cloud can be seen. This white cloud was assumed to be layer of Ta<sub>2</sub>O<sub>5</sub> that this not dissolve properly to form nanotubular shape. Although the structures improved, the nanotubular shapes were very thin. Besides that, Fig. 4(G2) shows that sample changed into silver colour and the surface was smooth. Here, we discovered

that silver colour on sample can be determine as a sign that anodization is performing properly and nanostructure Ta<sub>2</sub>O<sub>5</sub> is starting to take shape.

To further prove this fact, we conducted XRD analysis on sample G. Other than providing information on crystalline quality, XRD also provided orientation of nanostructure on metal oxide. Fig. 5 illustrated the XRD pattern for sample G after annealing. Interestingly, it exhibited the crystalline phase according to JCPDS file no. 25-0922, where diffraction peaks can be seen at 22.9, 28.3, 36.7, 46.7, 49.7, 55.5, 58.5, 63.6 and 70.5° 2-theta. The peaks fitted well with orthorhombic Ta<sub>2</sub>O<sub>5</sub>. However, diffraction peaks also appeared at 69.6° 2-theta which fitted well with cubic Ta. This result supported that 4 vol% of H<sub>2</sub>O starting to produce nanotubular Ta<sub>2</sub>O<sub>5</sub> but thin.

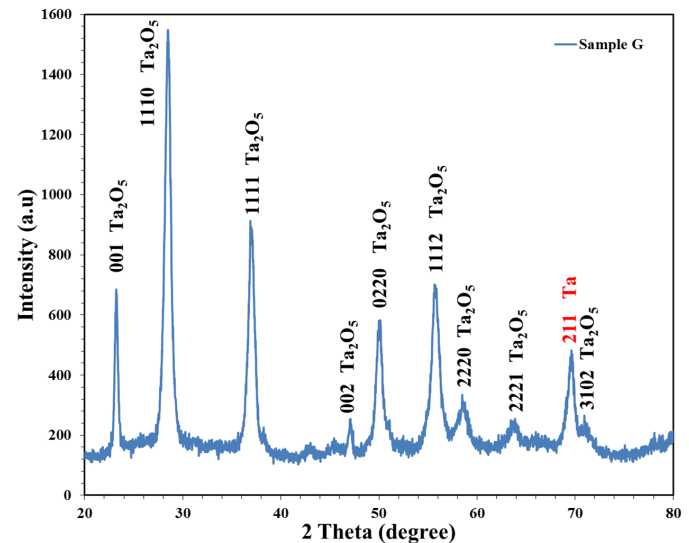


Fig. 5 XRD pattern of sample anodized in electrolyte with 4 vol% of H<sub>2</sub>O (sample G) after annealing at 500 °C for 2 h. Diffraction peaks appeared at 22.9, 28.3, 36.7, 46.7, 49.7, 55.5, 58.5, 63.6 and 70.5° 2-theta as orthorhombic Ta<sub>2</sub>O<sub>5</sub> and 69.6° 2-theta as cubic Ta.

**Table 2**

Summary of the anodization experiments with different concentration of H<sub>2</sub>O.

Experiment	EG (ml)	NH <sub>4</sub> F (wt%)	H <sub>2</sub> O (vol%)	H <sub>2</sub> SO <sub>4</sub> (vol%)	Observation
Baseline	50	3.0	10	0.25 H <sub>3</sub> PO <sub>4</sub>	
Sample E	50	1.35	0	0.25	No structure. Silver colour Rough surface
Sample F	50	1.35	2.0	0.25	Pore structure. Pinkish colour Rough surface
Sample G	50	1.35	4.0	0.25	Thin nanotubular Pinkish colour Smooth surface
Sample H	50	1.35	6.0	0.25	Damaged structure Pinkish colour Rough surface

We decided to slightly increase the volume H<sub>2</sub>O to 6 vol%. However, nanotubular appears to be damage in the presence of higher concentration of H<sub>2</sub>O (Fig. 4(H1)) even though the condition of the sample was smooth (Fig. 4(H2)). These results lead to conclusion where by controlling and slightly adding the amount of H<sub>2</sub>O not more or less than 4 vol% contributes in increasing the dissolution rate, overcome the limitation of continuous dissolution and form thicker nanotubular Ta<sub>2</sub>O<sub>5</sub>. Table 2 provides the summary of these experiments.

C. Optimization of H<sub>2</sub>SO<sub>4</sub> concentration in electrolyte

Prior research suggest that the use of acid in anodization is necessary to produce nanostructure metal oxide [32], [39]. In addition, previous studies have emphasized that nanotubular Ta<sub>2</sub>O<sub>5</sub> can be produced specifically with concentrated H<sub>2</sub>SO<sub>4</sub> [31], [40].

H<sub>2</sub>SO<sub>4</sub> solutions with different concentration possess different acidity, which leads to different chemical dissolution of tantalum and influence the equilibrium between electrochemical formation of tantalum and chemical dissolution of tantalum. It is expected that no nanotubular Ta<sub>2</sub>O<sub>5</sub> could be formed in the electrolyte with acidity that is too high or too low.

The effect of H<sub>2</sub>SO<sub>4</sub> on nanotubular formation was study by using 0 vol% (sample I), 0.5 vol% (sample J), 0.75 vol% (sample K) and 1.0 vol% (sample L) of H<sub>2</sub>SO<sub>4</sub> in electrolyte. The concentrations of EG (50 mL), NH<sub>4</sub>F (1.35 wt%) and H<sub>2</sub>O (4.0 vol%) in electrolyte was consistence. From Fig. 6(I1), no nanostructures can be observed when Ta film is anodized without the presence of H<sub>2</sub>SO<sub>4</sub>. To boot, there was no significant color change on the sample (Fig. 6(I2)). Results in Fig. 6(J1) and (J2) demonstrated that nanotubular Ta<sub>2</sub>O<sub>5</sub> cannot be produce without the present of H<sub>2</sub>SO<sub>4</sub>.

On the other hand, nanotubular Ta<sub>2</sub>O<sub>5</sub> with less prominent white cloud can be observed when anodized in 0.5 vol% of H<sub>2</sub>SO<sub>4</sub>, as seen in Fig. 6(J1). The voids and tubes of nanotubulars were very obvious. Notably, sample changed into smooth deep silver colour (Fig. 6(J2)). This shows that dissolution rate by localized acidification were adjusted properly with 0.5 vol% of H<sub>2</sub>SO<sub>4</sub>.

We conducted XRD analysis on sample J. Fig. 7 illustrated the XRD pattern for sample J after annealing. As expected, it exhibited a crystalline phase according to JCPDS file no. 25-0922, where diffraction peaks can be seen at 22.9, 28.3, 36.7, 46.7, 49.7, 55.5, 58.5, 63.6, 69.3 and 70.5° 2-theta. The peaks fitted well with orthorhombic Ta<sub>2</sub>O<sub>5</sub>. In comparison with previous XRD result on sample G, diffraction peaks of crystalline phase were higher and no diffraction peaks of cubic Ta can be seen. This result supported that 0.5 vol% of H<sub>2</sub>SO<sub>4</sub> produced thicker nanotubular Ta<sub>2</sub>O<sub>5</sub> layer.

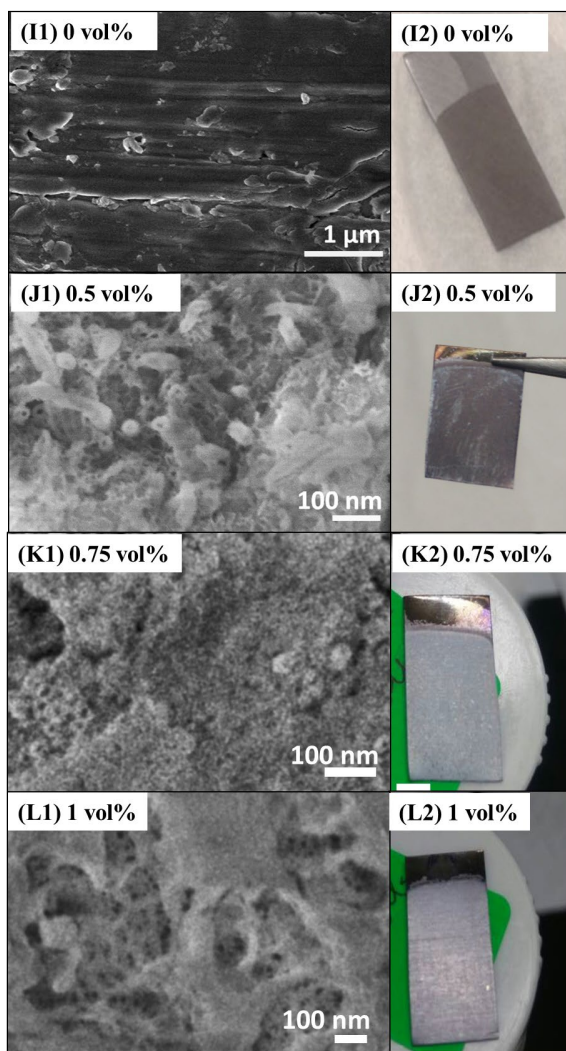


Fig. 6 FESEM and samples images after anodization in different concentration of H<sub>2</sub>SO<sub>4</sub>; (I1)(I2) 0 vol% H<sub>2</sub>SO<sub>4</sub>, (J1)(J2) 0.5 vol% H<sub>2</sub>SO<sub>4</sub>, (K1)(K2) 0.75 vol% H<sub>2</sub>SO<sub>4</sub>, (L1)(L2) 1 vol% H<sub>2</sub>SO<sub>4</sub>.

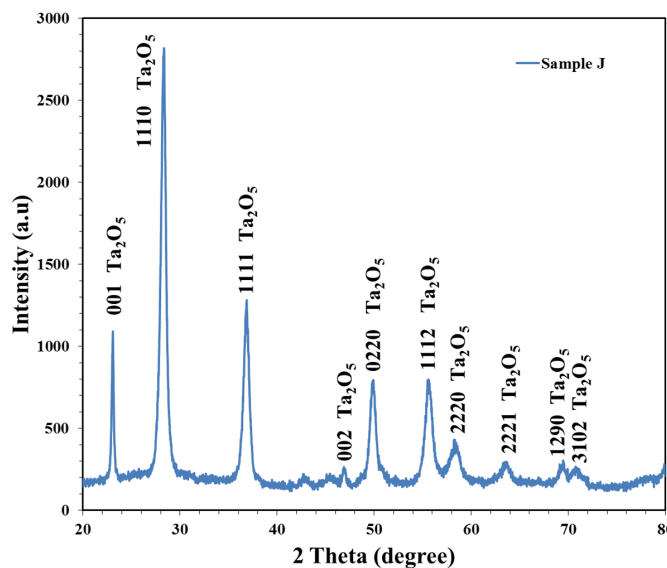


Fig. 7 XRD pattern of sample anodized in electrolyte with 0.5 vol% of H<sub>2</sub>SO<sub>4</sub> (sample J) after annealing at 500 °C for 2 h. Diffraction peaks appeared at 22.9, 28.3, 36.7, 46.7, 49.7, 55.5, 58.5, 63.6, 69.3 and 70.5° 2-theta as orthorhombic Ta<sub>2</sub>O<sub>5</sub>.

Contrary to findings of Fig. 6(J1) and (J2), nanotubular can be observed but random, imperfect and thinner when concentration of H<sub>2</sub>SO<sub>4</sub> increased to 0.75 vol%, (Fig. 6(K1)). Sample changed into brighter silver colour and slightly rough (Fig. 6(K2)). A difference result between 0.5 vol% and 0.75 vol% of H<sub>2</sub>SO<sub>4</sub> can be attributable to dissolution rate which assumed to be affected by high concentration of acid in electrolyte. 0.75 vol% of H<sub>2</sub>SO<sub>4</sub> was deemed to disturb the steady state of nanotubular formation.

Fig. 6(L1) further proven that concentration higher than 0.5 vol% effect the formation of nanotubular. Similarly, nanotubular structures were random, imperfect and thinner. Only pores can be seen, while tubes did not exist. Surface of the sample was rougher (Fig. 6(L2)) compare to Fig. 6(K2). The summary of these experiments is shown in Table 3

**Table 3**

*Summary of the anodization experiments with different concentration of H<sub>2</sub>SO<sub>4</sub>*

Experiment	EG (ml)	NH <sub>4</sub> F (wt%)	H <sub>2</sub> O (vol%)	H <sub>2</sub> SO <sub>4</sub> (vol%)	Observation
Baseline	50	3.0	10	0.25	
Sample I	50	1.35	4.0	0	No structure. No colour change
Sample J	50	1.35	4.0	0.5	Thicker nanotubular Deep silver colour Smooth surface
Sample K	50	1.35	4.0	0.75	Random, thin nanotubular Silver colour Rough surface
Sample L	50	1.35	4.0	1.0	Pore structure Silver colour Rough surface

#### D. Growth mechanism of nanotubular Ta<sub>2</sub>O<sub>5</sub> structure

Based on our discussion in previous chapter, the physical and chemical properties of nanotubular layers can be controlled by changing the parameters of fabrication process, mainly the concentration of electrolyte mixture. Concentration of electrolyte mixture affected the pH of electrolyte. The pH of electrolyte is an important factor to achieve high-aspect ratio nanotubular. The pH difference leads to significant pore diameter variations. Differences in thickness are attributed to the pH dependency of the oxide dissolution rate, in which previous study shows that the low pH dissolution rate is much higher than the higher pH. The formation of hydrolysis products at the working electrode leads to a decrease in pH; local acidification is therefore established. Adjusting the local acidification could promote the dissolution of Ta<sub>2</sub>O<sub>5</sub>, thus providing a more protective environment against dissolution along the tube mouth, and longer tubes were thus obtained.

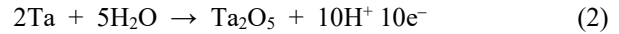
Based on the observation and reports of the growth mechanism of the nanotubular Ta<sub>2</sub>O<sub>5</sub>, the evolving process of the nanotubular is shown in Fig. 8 and Fig. 9. Before anodization start, initially a tantalum oxide passivation layer is

formed on Ta foil through hydrolysis of tantalum. In the electrolyte, oxide layer is formed when a constant voltage is applied. The formation of the nanotubular in NH<sub>4</sub>F, which is the source of fluoride ion in electrolyte, is due to two competing electric field-assisted processes. These two processes are as follow; (i) hydrolysis of Ta to form Ta<sub>2</sub>O<sub>5</sub> and (ii) chemical dissolution of Ta<sub>2</sub>O<sub>5</sub> at the oxides/electrolyte interfaces (Fig. 8). Fluoride ion (F<sup>-</sup>) is fundamental factor for the development of tubular structure due to its ability to form soluble [TaF<sub>7</sub>]<sup>2-</sup>. Moreover, its small ionic radius makes them suitable to penetrate into the growing Ta<sub>2</sub>O<sub>5</sub> lattice, thus transported through the oxide by applied field. Precisely, it has a role as an oxide dissolution agent. The reactions to nanotubular formation are given below;

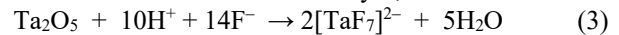
Oxidation of Ta;



Formation of oxide layer (hydrolysis);



Chemical dissolution of oxide layer;



Eq. 1 illustrates the oxidation of Ta into Ta<sup>5+</sup>. As seen in Eq. 2, H<sup>+</sup> increased during hydrolysis, and then F<sup>-</sup> ions travel to the sites of H<sup>+</sup> to achieve electroneutrality. Eventually, F<sup>-</sup> ions compete for the sites of O<sup>2-</sup> in the oxide. Next, the dissolution of Ta<sub>2</sub>O<sub>5</sub> happened by the formation of [TaF<sub>7</sub>]<sup>2-</sup> when concentration of H<sup>+</sup>, F<sup>-</sup> and O<sup>2-</sup> reached a critical level at local regions, as shown in Eq. 3. Dissolution of Ta creates negatively charged cation vacancies at the oxide and migrates to the metal/oxide interface as a result of potential gradient across the oxide. The existence of metal cation vacancies near the metal /oxide interface promotes the reaction in Eq. 1 and the Ta<sup>5+</sup> jumps easily to the vacancy sites available. Furthermore, nanopores were nucleated on the oxide surface during this state.

A mass of H<sup>+</sup> ions are generated at the bottom of the pore where the Ta came out of the metal and dissolved in the solution and the concentration of HF inside the pores increases rapidly. High concentration of HF causing the wall of pores dissolves until the adjacent pore walls disappear. In meantime, the integration by small pores resulted in the same appearance of larger pores. Synchronously, the enhanced electric field-assisted dissolution at the pore bottom deepening the pore and forming the voids. Due to the applied electric field, the Ta-O bond undergoes polarization and weakened which promotes the dissolution of the metal oxide. The pore bottom is self-acidified due to the electrochemical dissolution of Ta. This leads to the formation of pH profile in the growth direction of the pore. As a result, the dissolution rate at the pore bottom is higher than at the pore top, which increases the length of the nanotubular along with time.

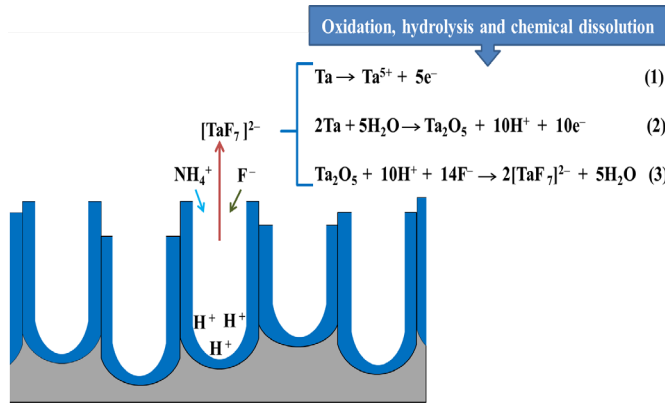


Fig. 8 The schematic shows the equation and reaction involved in formation of nanotubular Ta<sub>2</sub>O<sub>5</sub>.

Briefly, the mechanism of nanotubular can be concluded as following; (a) oxide layer formation, (b) formation and deepening of pore, (c) initial nanotubular formation and (d) perfect formation of nanotubular. Fig. 9 shows the summary of nanotubular growth mechanism.

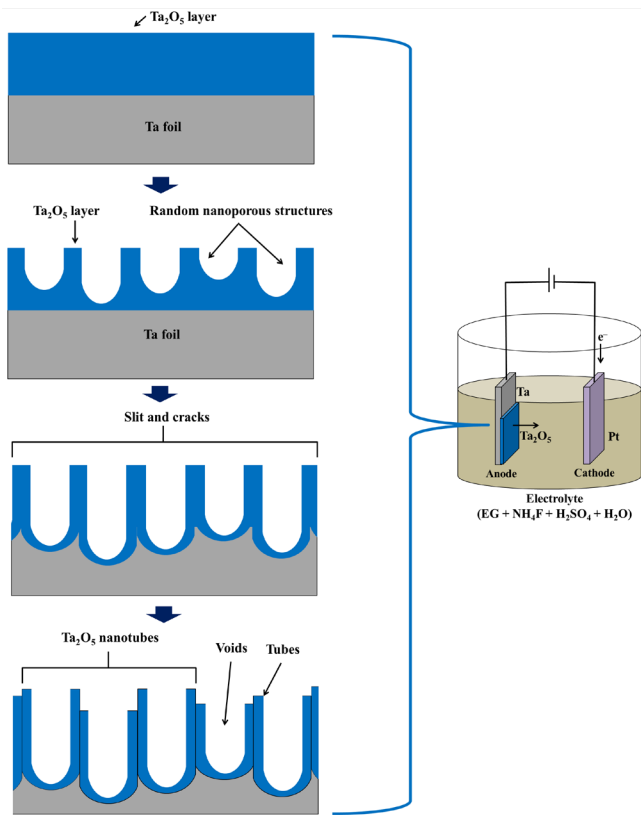


Fig. 9 This schematic illustrates the step by step mechanism formation of nanotubular Ta<sub>2</sub>O<sub>5</sub>

#### IV. CONCLUSION

Nanotubular Ta<sub>2</sub>O<sub>5</sub> can be produced in an exceptionally controlled condition by electrochemical anodization in ethylene glycol solution with addition of acid sulphuric, ammonium fluoride and water. Optimized concentration of NH<sub>4</sub>F (1.35 wt%) plays a major role in pore formation and dissolution. Experimental results uncovered that addition of water (4 vol%) accelerate chemical dissolution of Ta<sub>2</sub>O<sub>5</sub>. Our results also revealed that chemical dissolution of Ta<sub>2</sub>O<sub>5</sub> with H<sub>2</sub>SO<sub>4</sub> (0.5 vol%) presence in electrolyte plays a key role in the formation of nanotubular. Finally, crystallographic structures show that thermal treatment (annealing) at high temperature of 500 °C change Ta<sub>2</sub>O<sub>5</sub> morphology from amorphous to crystalline phase.

#### ACKNOWLEDGEMENT

The authors would like to thank the Research Management Institutes (RMI) of UiTM for their support on this research. The authors would also like to thank the NANO-ElecTronic Center (NET), Faculty of Electrical Engineering, UiTM for the use of their laboratory and Faculty of Applied Sciences, UiTM for the use of their XRD facility.

#### REFERENCES

- [1] A. F. Feil, M. V da Costa, P. Migowski, J. Dupont, S. R. Teixeira, and L. Amaral, "From alumina nanopores to nanotubes: dependence on the geometry of anodization system," *J. Nanosci. Nanotechnol.*, vol. 11, no. 3, pp. 2330–2335, 2011.
- [2] S. Dadras and M. Faraji, "Improved carbon nanotube growth inside an anodic aluminum oxide template using microwave radiation," *J. Phys. Chem. Solids*, vol. 116, no. July 2017, pp. 203–208, 2018.
- [3] T. Li, K. Gulati, N. Wang, Z. Zhang, and S. Ivanovski, "Understanding and augmenting the stability of therapeutic nanotubes on anodized titanium implants," *Mater. Sci. Eng. C*, vol. 88, no. 2017, pp. 182–195, 2018.
- [4] K. R. Hebert, *Kinetics of Anodic Oxidation of Aluminum and Titanium: Formation of Porous Alumina and Titanium Oxide Nanotube Layers*. Elsevier, 2017.
- [5] N. I. Soaid, N. Bashirom, M. Rozana, and Z. Lockman, "Formation of anodic zirconia nanotubes in fluorinated ethylene glycol electrolyte with K<sub>2</sub>CO<sub>3</sub> addition," *Surf. Coatings Technol.*, vol. 320, pp. 86–90, 2017.
- [6] X. Li, H. Xu, Y. Jin, and T. Zhang, "Fabrication of highly ordered nanotube layer on Zr-based bulk metallic glass for biomedical uses," *Mater. Lett.*, vol. 200, pp. 63–66, 2017.
- [7] M. Yang *et al.*, "A new electrochemical platform for ultrasensitive detection of atrazine based on modified self-ordered Nb<sub>2</sub>O<sub>5</sub> nanotube arrays," *J. Electroanal. Chem.*, vol. 791, pp. 17–22, 2017.
- [8] C. Shi, K. Xiang, Y. Zhu, X. Chen, W. Zhou, and H. Chen, *Preparation and electrochemical properties of nanocable-like Nb<sub>2</sub>O<sub>5</sub>/surface-modified carbon nanotubes composites*

- for anode materials in lithium ion batteries, vol. 246. Elsevier Ltd, 2017.
- [9] L. Li, X. Zhao, D. Pan, and G. Li, "Nanotube array-like WO<sub>3</sub>/W photoanode fabricated by electrochemical anodization for photoelectrocatalytic overall water splitting," *Cuihua Xuebao/Chinese J. Catal.*, vol. 38, no. 12, pp. 2132–2140, 2017.
- [10] S. Caramori, V. Cristino, L. Meda, A. Tacca, R. Argazzi, and C. A. Bignozzi, "Efficient anodically grown WO<sub>3</sub> for photoelectrochemical water splitting," *Energy Procedia*, vol. 22, pp. 127–136, 2011.
- [11] A. Kohlsdorf, D. H. Taffa, and M. Wark, "Journal of photochemistry and photobiology A : chemistry microwave assisted synthesis of Ta<sub>2</sub>O<sub>5</sub> nanostructures for photocatalytic hydrogen productio n," *Journal Photochem. Photobiol. A Chem.*, 2018.
- [12] A. A. Ismail, M. Faisal, F. A. Harraz, A. Al-Hajry, and A. G. Al-Sehemi, "Synthesis of mesoporous sulfur-doped Ta<sub>2</sub>O<sub>5</sub> nanocomposites and their photocatalytic activities," *J. Colloid Interface Sci.*, vol. 471, pp. 145–154, 2016.
- [13] P. Gibot, F. Schnell, and D. Spitzer, "Synthesis of Nb<sub>2</sub>O<sub>5</sub> and Ta<sub>2</sub>O<sub>5</sub> nanopowders by means of an endo-templating method," *Ceram. Int.*, vol. 43, no. 18, pp. 16451–16456, 2017.
- [14] J. Li, W. Dai, G. Wu, N. Guan, and L. Li, "Fabrication of Ta<sub>2</sub>O<sub>5</sub> films on tantalum substrate for efficient photocatalysis," *Catal. Commun.*, vol. 65, pp. 24–29, 2015.
- [15] K. Sawangsri *et al.*, "Experimental band alignment of Ta<sub>2</sub>O<sub>5</sub>/GaN for MIS-HEMT applications," *Microelectron. Eng.*, vol. 178, pp. 178–181, 2017.
- [16] N. Samsudin *et al.*, "Deposition and characterization of RF-sputtered-Ta<sub>2</sub>O<sub>5</sub> thin films for O<sub>2</sub> reduction reaction in polymer electrolyte membrane fuel cells (PEMFC)," *Optik (Stuttg.)*, vol. 170, no. May, pp. 295–303, 2018.
- [17] T. Wahlbrink *et al.*, "Fabrication and characterization of Ta<sub>2</sub>O<sub>5</sub> photonic feedback structures," *Microelectron. Eng.*, vol. 85, no. 5–6, pp. 1425–1428, 2008.
- [18] A. Baruah, M. Jha, S. Kumar, and A. K. Ganguli, "Enhancement of photocatalytic efficiency using heterostructured SiO<sub>2</sub>–Ta<sub>2</sub>O<sub>5</sub> thin films," *Mater. Res. Express*, vol. 2, no. 5, p. 056404, 2015.
- [19] S. Kim, "Hydrogen gas sensors using a thin Ta<sub>2</sub>O<sub>5</sub> dielectric film," *J. Korean Phys. Soc.*, vol. 65, no. 11, pp. 1749–1753, 2014.
- [20] R. Kant, R. Tabassum, and B. D. Gupta, "A highly sensitive and distinctly selective D-sorbitol biosensor using SDH enzyme entrapped Ta<sub>2</sub>O<sub>5</sub> nanoflowers assembly coupled with fiber optic SPR," *Sensors Actuators, B Chem.*, vol. 242, pp. 810–817, 2017.
- [21] Y. Li, K. Nagato, J. J. Delaunay, J. Kubota, and K. Domen, "Fabrication of highly ordered Ta<sub>2</sub>O<sub>5</sub> and Ta<sub>3</sub>N<sub>5</sub> nanorod arrays by nanoimprinting and through-mask anodization," *Nanotechnology*, vol. 25, no. 1, 2014.
- [22] D. Ding, Y. Xie, K. Li, L. Huang, and X. Zheng, "Black plasma-sprayed Ta<sub>2</sub>O<sub>5</sub> coatings with photothermal effect for bone tumor therapy," *Ceram. Int.*, vol. 44, no. 11, pp. 12002–12006, 2018.
- [23] J. Xu, X. ke Bao, T. Fu, Y. Lyu, P. Munroe, and Z. H. Xie, "In vitro biocompatibility of a nanocrystalline β-Ta<sub>2</sub>O<sub>5</sub> coating for orthopaedic implants," *Ceram. Int.*, vol. 44, no. 5, pp. 4660–4675, 2018.
- [24] E. Atanassova, D. Spassov, and A. Paskaleva, "Influence of the metal electrode on the characteristics of thermal Ta<sub>2</sub>O<sub>5</sub> capacitors," *Microelectron. Eng.*, vol. 83, no. 10, pp. 1918–1926, 2006.
- [25] E. Atanassova, D. Spassov, A. Paskaleva, M. Georgieva, and J. Koprinarova, "Electrical characteristics of Ti-doped Ta<sub>2</sub>O<sub>5</sub>stacked capacitors," *Thin Solid Films*, vol. 516, no. 23, pp. 8684–8692, 2008.
- [26] A. Abouelsayed, W. H. Eisa, M. Dawy, and A. Shabaka, "Ultraviolet and infrared studies of the single-walled and multi-walled carbon nanotube films with different thickness," *Phys. B Condens. Matter*, vol. 483, pp. 8–12, 2016.
- [27] X. Zu *et al.*, "Self-powered UV photodetector based on heterostructured TiO<sub>2</sub> nanowire arrays and polyaniline nanoflower arrays," *Synth. Met.*, vol. 200, pp. 58–65, 2015.
- [28] R. A. Rani, A. S. Zoolfakar, J. Z. Oua, M. R. Field, M. Austin, and K. Kalantar-Zadeh, "Nanoporous Nb<sub>2</sub>O<sub>5</sub> hydrogen gas sensor," *Sensors Actuators, B Chem.*, vol. 176, pp. 149–156, 2013.
- [29] R. Ab Kadir *et al.*, "Optical gas sensing properties of nanoporous Nb<sub>2</sub>O<sub>5</sub> films," *ACS Appl. Mater. Interfaces*, vol. 7, no. 8, pp. 4751–4758, 2015.
- [30] N. Verma, K. C. Singh, B. Mari, M. Mollar, and J. Jindal, "Anodic oxide films on niobium and tantalum in different aqueous electrolytes and their impedance characteristics," *Acta Phys. Pol. A*, vol. 129, no. 3, pp. 297–303, 2016.
- [31] N. K. Allam, X. J. Feng, C. A. Grimes, N. K. Allam, X. J. Feng, and C. A. Grimes, "Self-assembled fabrication of vertically oriented Ta<sub>2</sub>O<sub>5</sub> nanotube arrays and membranes thereof, by one-step tantalum anodization," *Chem. Mater.*, vol. 20, pp. 6477–6481, 2008.
- [32] R. V. Gonçalves *et al.*, "Ta<sub>2</sub>O<sub>5</sub> nanotubes obtained by anodization: effect of thermal treatment on the photocatalytic activity for hydrogen production," *J. Phys. Chem. C*, vol. 116, no. 26, pp. 14022–14030, 2012.
- [33] R. V. Gonçalves *et al.*, "Catalytic abatement of CO over highly stable Pt supported on Ta<sub>2</sub>O<sub>5</sub> nanotubes," *Catal. Commun.*, vol. 48, pp. 50–54, 2014.
- [34] M. M. Momeni, M. Mirhosseini, and M. Chavoshi, "Fabrication of Ta<sub>2</sub>O<sub>5</sub> nanostructure films via electrochemical anodisation of tantalum," vol. 00, no. 0, pp. 1–7, 2015.
- [35] H. Yu, S. Zhu, X. Yang, X. Wang, H. Sun, and M. Huo, "Synthesis of coral-like tantalum oxide films via anodization in mixed organic-inorganic electrolytes," *PLoS One*, vol. 8, no. 6, pp. 6–11, 2013.
- [36] H. H. H. Hareith I. Jaafar, Abdulkareem M. a. Alsammerraei, "Study of the effect of NH<sub>4</sub>F concentration on the surface of electrochemically prepared TiO<sub>2</sub> nanotubes," *Iraqi J. Sci.*, vol. Vol 53, no. ..No 2, pp. 827–831, 2012.
- [37] J. Z. Ou *et al.*, "Elevated temperature anodized Nb<sub>2</sub>O<sub>5</sub>: A photoanode material with exceptionally large photoconversion efficiencies," *ACS Nano*, vol. 6, no. 5, pp. 4045–4053, 2012.
- [38] W. Wei, J. M. Macak, and P. Schmuki, "High aspect ratio ordered nanoporous Ta<sub>2</sub>O<sub>5</sub> films by anodization of Ta," *Electrochem. commun.*, vol. 10, no. 3, pp. 428–432, 2008.
- [39] R. V. Gonçalves *et al.*, "On the crystallization of Ta<sub>2</sub>O<sub>5</sub> nanotubes: structural and local atomic properties investigated by EXAFS and XRD," *CrystEngComm*, vol. 16, no. 5, p. 797, 2014.
- [40] H. A. El-Sayed and V. I. Birss, "Controlled growth and monitoring of tantalum oxide nanostructures," *Nanoscale*, vol. 2, no. 5, p. 793, 2010.